

Study of the mineralization potential of the intrusives around Valis (Tarom-Iran)

Mojtaba Bahajroy¹, Saeed Taki^{1,2}
email: Taki_Saeed2002@yahoo.com

1&2: Department of Geology, Lahijan Branch, College of Basic Sciences, Islamic Azad University, Lahijan, Iran.

ABSTRACT

The study area is located in northwestern Iran in the central Iran zone, specifically the western Alborz sub-zone south of the Tarom-Hashitjin metallogenic zone. The exposed rock units in this area generally include Eocene volcanic rocks (lava flows and pyroclasts belonging to the Karaj formation) and Oligocene granitoid intrusive bodies. The intrusive bodies in the area have a petrographic composition of granite, syenite and monzonite and are mostly metaluminous. The dual characteristics of these intrusives (for example, the behavior of elements such as Rb, P, Ga/Al, Y/Nb, K/Na, and FeO/Fe₂O₃, the Rb/Nb ratios, the A/CNK molar ratios and the ACF and A/CNK-Fe₂O₃+FeO diagrams), some of which are consistent with the I nature and others with the S and A natures, show that the rocks are among hybrid granitoids and, in terms of the tectonic setting, lie within the WPG range. According to the Rb/Sr, Zr/Hf, K/Rb ratios, the granite melts that form the aforementioned bodies are not extremely evolved and have not undergone post magmatic activity, which would lead to mineralization. The Sm/Eu and Rb/Ba ratios and the behavior of Rb, Ba and Sr within the aforementioned granitoids show that the rocks are similar to average granitoids unrelated to Li, Be, Sn, W and Ta deposits; they fall within the range of barren granitoids but are partially fertile in Cu.

Key words: Intrusive, Valis, Tarom, Hybrid, Barren.

RESUMEN

El área de este estudio está localizada en el noroeste de la zona central de Irán, específicamente en el oeste de la subzona de Alborz y al sur de la zona metalogénica de Tarom-Hashitjin. Las unidades de roca expuesta en esta área se clasifican generalmente como rocas volcánicas del Eoceno (flujos de lava y piroclastos pertenecientes a la formación Karaj) y como cuerpos granitoides intrusivos del Oligoceno. Los cuerpos intrusivos en el área tienen una composición petrográfica de granito, sienita y monzonita mayormente metaluminosa. Las características duales de estas intrusiones (por ejemplo, el comportamiento de elementos como Rb, P, Ga/Al, Y/Nb, K/Na, y Feo/Fe₂O₃, los índices de Rb/Nb, la proporción molar de los A/CNK y los diagramas ACF y A/CNK-Fe₂O₃+FeO), algunas de las cuales son consistentes con la índole I y otras con las índoles S y A, muestran que las rocas son granitoides híbridos y, en términos de orden tectónico, subyacen en la cadena WPG. De acuerdo con los índices Rb/Sr, Zr/Hf, K/Rb, los granitos fundieron la forma de los cuerpos sin desarrollarse completamente y sin registrar actividad magmática posterior, lo que llevó a la mineralización. Los índices Sm/Eu y Rb/Ba y el comportamiento del Rb, Ba y Sr al interior de los granitoides mencionados muestran que las rocas son similares al promedio de los granitoides no relacionados con los depósitos de Li, Be, Sn, W y Ta; estos se incluyen en el rango de granitoides estériles, pero son parcialmente fértiles en Cu.

Palabras clave: Intrusión, Valis, Tarom, híbrido, estéril.

Record

Manuscript received: 06/08/2014
Accepted for publication: 09/09/2014

Introduction

The study area is located in northwestern Iran and is part of the Alborz mountain range. Alborz itself is affected by the Alp-Himalayan orogeny and generally trends northwest-southeast. This area is geographically located between the eastern longitudes of $48^{\circ} 30'$ to $48^{\circ} 40'$ and northern latitudes of 37° to $37^{\circ} 5'$. In terms of Iran's structural division, this area is located in the western Alborz subzone in central Iran (Alavi, 1996) (figure 1), and from metallogenic point of view, it belongs to the multimetallic belt of Taron-Hashtjin (Ghorbani, 2013). The Taron-Hashtjin belt covers an area between Qazvin (west of Taleghan) and north-northwest of Mianeh; it is limited by the Manjil depression and Talesh Mountains to the north and by the Alborz-Zanjan-Mianeh axis to the south. In fact, this belt is structurally confined to the north by the Sefidrood fault, to the south by the continuation of the Tabriz-Soltanieh and Soltanieh-Takestan faults, and to the west by the Astara-Marivan fault (Ghorbani, 2013) (figure 1).

Almost the entire study area is composed of Cenozoic volcanic, intrusive, and sedimentary rocks. The rocks along the Taron-Hashtjin axis, which are considered equivalent to the Karaj Formation, are different from those in central Alborz in terms of the lithology and chemical composition because the lava flows do not consist only of volcanoclastic rocks along this axis and their compositions are more basic. In fact, the rocks in the Karaj Formation in central Alborz are predominantly acidic tuffs, while their equivalents along the Taron-Hashtjin axis are mostly andesites and basaltic andesites. The ancient rocks in the Taron-Hashtjin belt are not exposed within the central parts (Ghorbani, 2013), and the basement is mostly composed of Tertiary magmatic rocks. The volcanic rocks in the Taron area vary from rhyodacite and dacite to basalt. These rocks are observed in the form of lava flows, tuffs and sometimes tuffites. According to the conducted studies, the following volcanic rocks have been observed in this belt: basalt, basaltic andesite, andesite, trachyte, latite, trachyandesite, dacite and rhyodacite ignimbrite and acidic to intermediate tuffs. Among these rocks, andesites are the most voluminous. Moein-Vaziri (1985) believed that most volcanic rocks from the Taron-Hashtjin are potassic-alkaline, while some are sodic-alkaline or calc-alkaline. Most of the andesites are shoshonitic.

The emplacement of Oligocene age acidic to intermediate intrusive bodies within the Eocene volcanic rocks and the existence of the mining indices of Zehabad, Barikabad, Khalifehlu, Aliabad and Golouje in the Taron region along with vast alteration zones have caused this area to be geologically considered as a prime geological district for the detection and identification of metallic and non-metallic deposits (Ghorbani, 2013). The studies conducted by different researchers (Peyrovan H., 1992; Torkamani E., 1997; Moayyed M., 2001) show that the granitoid bodies in this zone are of the I type. Haj Alilou (2000) believed that the intrusive bodies have been emplaced at a depth between 1400 to 3000 m and their formation temperature ranged from 700 to 880 degrees centigrade. Because of the high water content and sulfur fugacity, the bodies managed to create very extensive hydrothermal alterations together with vein, veinlet and scattered mineralizations in tuffites and Eocene volcanic rocks. The magmatic series of these intrusive bodies are shoshonite and high K calc-alkaline and are of the I type (Ghorbani, 2013). Shallower bodies are observed in the form of porphyry with the general composition of monzonite porphyry and occurred along with major bodies with important roles in mineralization and hydrothermal alteration. The structural geology features similar anticline and syncline axes, and faults trending east-west and northwest-southeast had important roles in the emplacement of intrusive bodies and the development of hydrothermal alteration areas. Sericitic, argillic (advanced, intermediate and weak), silicic, chloritic, propylitic, zeolitic and alunite alteration zones have been recognized along this axis.

The igneous bodies, which have economic concentrations of either genetic or paragenetic chemical elements, generally show specific geochemical patterns (Beus, 1968), the identification of which potentially distinguishes metalliferous geological units from barren types. When determining the mineralization potential of felsic intrusive bodies, it is important to recognize

their nature, which generally accompanies special types of ore deposits. To achieve this purpose and determine the mineralization ability of the granitoid bodies around Valis, petrography, petrology, and geochemical ratios and the distribution of major and rare elements have been studied; in addition, this granitoid body was compared with the world's most well-known fertile and barren granitoid bodies.

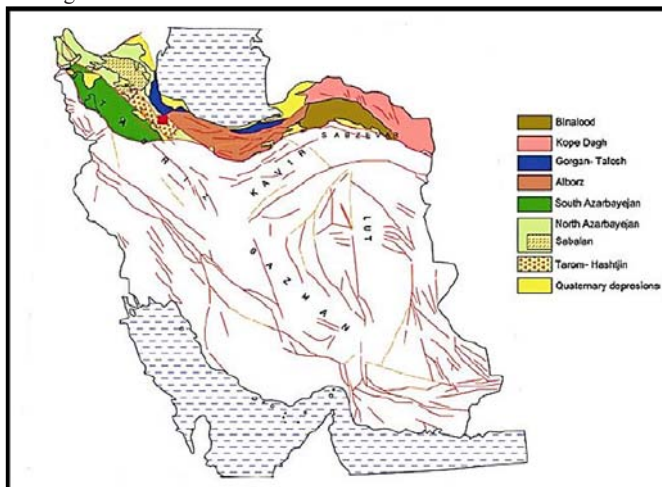


Figure 1. Location of the study area (red square) on Iran's structural divisions map (Alavi, 1996). This area is located in Alborz in the Taron-Hashtjin metallogenic zone according to the structural zoning implemented by Ghorbani (2013).

Geological Setting

This area is separated from the Talesh Mountains by Manjil Basin and from the Soltanieh Mountains by the Zanjan-Abhar Plain. The rock units in the area mainly include Eocene volcanic rocks (lava flows and pyroclasts belonging to the Karaj formation) and Oligocene granitoid intrusive bodies (figure 2). The volcanoclastic succession lithology in Taron, as in other areas in Alborz, consists of green tuffs and shaly and sometimes calcareous intercalations. The Eocene volcanic rocks in the area include volcanoclastic and extrusive rocks. The extrusive rocks in this area include andesite, basaltic andesite, quartz trachyandesite and basalt, though the bulk of these rocks are basaltic andesites and quartz trachyandesite. Many intrusive bodies have been injected into Eocene volcanoclastic assemblages, so these bodies are post-Eocene (most likely Oligocene) in age. One characteristic of the Oligocene intrusive bodies is the creation of alteration areoles in Eocene volcanoclastics, and their hydrothermal phases have been generally accompanied by the formation of elements such as epithermal gold, copper, lead, zinc and kaolin. The main body is exposed at the surface in the form of a prolate batholith trending northwest-southeast. Subvolcanic bodies are mostly observed in dyke form. Most faults in the area generally trend northwest-southeast, but some faults trend northeast-southwest. The aforementioned bodies were injected along the structures and longitudinal faults in the highs in Taron. Most structures in this area follow the fault system so that a set of alteration zones occurs along the faults.

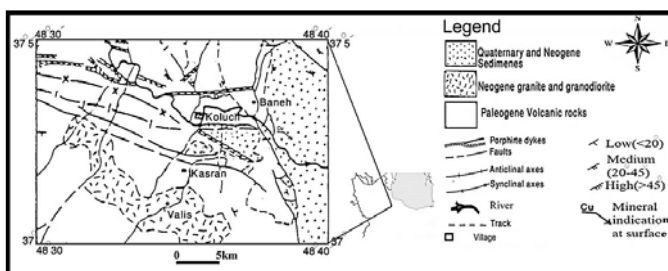


Figure 2. Simplified geological map of the study area (Davis et al, 1972).

Methodology

The rock samples were collected from the intrusive bodies in the study area. Forty-five thin sections were prepared for petrological study. To study the chemical characteristics, 11 of the most representative rock samples taken from the intrusives were selected for whole rock major oxide, trace element, and REE analysis and sent to ACME Company in Canada and the Atomic Energy Organization of Iran. At the ACME Company, the samples were first dried and then crushed and pulverized to pass a 200 mesh sieve. A lithium borate fusion and dilute nitric acid digestion of a 0.2 g sample pulp followed by ICP emission spectrometry was used to carry out the whole rock analysis for 11 major oxides and some minor elements. The loss on ignition (LOI) was obtained by sintering at 1000°C. Two separate ICP-MS analyses were done to determine the trace elements. The rare earth and refractory elements were collected from a lithium borate decomposition (same as that used for the major elements) to determine the total abundances. The precious and base metals and their associated pathfinder elements were generated from an aqua regia digestion (table 1). At the Atomic Energy Organization of Iran, the pulverized samples were mixed with boric acid and then pressed and analyzed using the XRF method (table 2). The geochemical data were processed using the Minpet 2.02 software. Because iron has been reported in its unseparated form, Irvine and Baragar's (1971) method was used in this study to calculate the bivalent and trivalent iron.

Table 1. Representative whole rock major oxides (wt %), trace elements (ppm) and rare earth elements (ppm) for samples from the intrusives around Valis (ICP-AES and ICP-MS) (implemented by the Acme Laboratory).

Sample no. Analyte	B1	B2	B3	B7	B8
SiO ₂	61.08	68.99	66.00	56.83	67.36
Al ₂ O ₃	15.30	14.34	14.50	16.33	14.64
Fe ₂ O ₃	5.58	3.11	3.82	6.29	3.59
MgO	1.38	0.65	1.08	3.39	0.46
CaO	1.78	1.63	2.01	7.45	1.52
Na ₂ O	2.64	3.01	3.58	3.29	3.22
K ₂ O	7.49	6.40	6.72	3.99	7.33
TiO ₂	0.75	0.46	0.56	0.94	0.58
P ₂ O ₅	0.18	0.09	0.12	0.35	0.10
MnO	0.61	0.14	0.14	0.23	0.08
Cr ₂ O ₃	0.007	0.019	0.006	0.011	0.019
Ni	20<	20<	20<	20<	20<
Sc	11	5	7	18	5
LOI	2.8	0.9	1.2	0.6	0.8
Sum	99.58	99.77	99.76	99.70	99.71
Ba	1293	286	676	672	481
Be	2	4	8	1<	6
Co	11.2	4.5	7.7	14.8	6.6
Cs	4.4	12.2	7.8	4.2	3.8
Ga	13.3	15.8	15.4	16.6	17.1
Hf	5.5	10.4	7.9	11.3	19.0
Nb	17.7	53.3	48.6	28.2	53.3
Rb	256.1	338.0	347.8	131.3	224.2
Sn	3	4	4	1	1<
Sr	277.1	210.3	197.1	492.1	307.9
Ta	1.3	3.8	3.9	2.0	3.5
Th	12.2	50.3	54.0	30.1	60.4
U	3.3	13.9	14.2	6.4	14.4
V	85	27	53	178	31
W	2.0	5.9	4.4	2.1	1.4
Zr	221.8	392.4	267.2	474.1	843.8
Y	20.8	36.4	35.3	32.1	26.2
La	37.5	55.7	40.8	34.6	26.2
Ce	66.3	105.8	76.7	69.0	46.5
Pr	7.36	11.78	8.19	8.42	5.40
Nd	27.5	42.2	28.7	32.0	20.6

Sm	4.70	6.79	5.40	6.49	4.22
Eu	1.14	0.63	0.93	1.06	0.68
Gd	4.39	6.50	5.58	6.54	4.31
Tb	0.63	0.95	0.88	0.94	0.65
Dy	3.97	5.92	5.60	5.86	3.94
Ho	0.80	1.22	1.25	1.20	0.85
Er	2.24	3.71	3.89	3.26	2.91
Tm	0.35	0.63	0.62	0.50	0.44
Yb	2.25	4.31	4.10	3.29	2.73
Lu	0.33	0.71	0.62	0.52	0.48
Mo	1.2	2.3	1.3	1.5	2.2
Cu	6.8	19.3	74.1	13.6	23.7
Pb	361.5	32.9	42.6	22.2	15.0
Zn	870	113	84	50	37
Ni	4.6	5.3	4.1	12.8	5.2
As	2.9	5.4	9.7	4.1	5.4
Cd	2.0	0.2	0.2	0.1<	0.1
Sb	0.6	2.0	2.8	0.6	1.6
Bi	0.1	0.1<	0.1<	0.1<	0.1<
Ag	0.1	0.1<	0.1	0.1<	0.1<
Au	1.8	1.0	1.1	0.5<	0.5<
Hg	0.01	0.01<	0.01<	0.01<	0.01<
Tl	0.1<	0.1<	0.1<	0.1<	0.1<
Se	0.5<	0.5<	0.5<	0.5<	0.5<

Table 2. Representative whole rock major oxides (wt %) and trace elements (ppm) for samples from the intrusives around Valis (XRF) (implemented by the Atomic Energy Organization of Iran).

Sample no. Analyte	HS-01	HS-02	HS-03	VA-04	VA-08	VA-11
SiO ₂	63.904	63.738	66.865	69.226	69.801	69.330
Al ₂ O ₃	16.003	15.844	15.231	13.751	14.430	14.578
Fe ₂ O ₃	3.361	3.520	3.037	2.312	2.357	2.214
CaO	3.194	3.376	2.19	1.778	1.445	1.855
Na ₂ O	3.023	3.057	3.024	2.826	3.022	1.921
MgO	1.025	1.165	0.771	0.786	0.428	0.727
K ₂ O	5.775	5.769	6.038	5.676	6.002	6.147
TiO ₂	0.511	0.527	0.457	0.329	0.324	0.333
MnO	0.066	0.071	0.058	0.042	0.067	0.035
P ₂ O ₅	0.166	0.170	0.127	0.089	0.088	0.087
Ba	531	530	368	236	334	316
Ce	66	55	77	116	74	45
CO	8	10	7	7	3	3
Cr	N	4	4	N	N	N
Cu	60	48	66	9	33	31
Nb	34	36	43	46	36	42
Ni	6	13	21	17	17	13
Pb	34	22	48	23	41	20
Rb	238	237	281	330	333	302
Sr	354	361	233	199	210	249
MO	4	3	5	5	5	5
V	57	61	49	38	36	38
Y	34	34	37	42	40	39
Zr	378	410	403	267	271	280
Zn	75	54	62	44	84	41
U	10	6	14	18	15	16
Th	29	22	47	55	50	46

Discussion and Results

Geochemistry and Tectonomagnetic Setting of the Intrusives around Valis

The petrographical studies and chemical classification diagrams show that the intrusive bodies in the study area have granite, syenite and monzonite (granitoid) compositions and are mostly metaluminous (figure 3). Contradictory features in the intrusives (such as the behavior of P, Rb, Ga/Al, Y/Nb, K/Na, and FeO/Fe₂O₃, the Rb/Nb ratios, the A/CNK molar ratios and the A/CNK-Fe₂O₃+FeO and ACF diagrams), some of which are consistent with the I nature and others with the S and A natures, show that the rocks are classified as hybrid granitoids (figures 4-7).

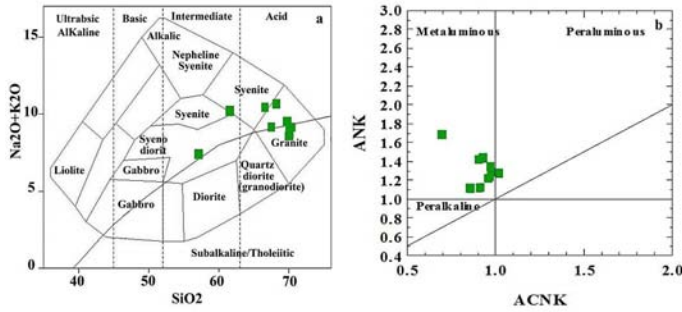


Figure 3. Plot of chemical data from the intrusives around Valis on a) chemical rock classification (Cox et al, 1971) and b) aluminum saturation index (Maniar and Piccoli, 1989) diagrams.

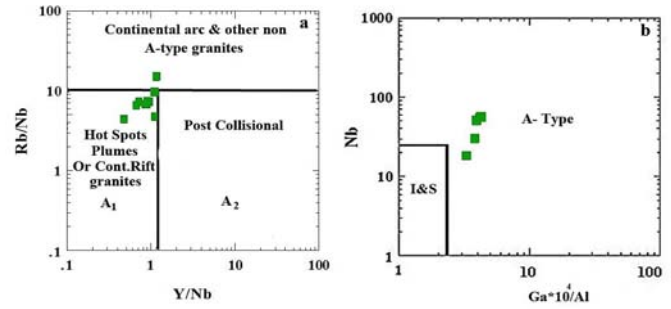


Figure 7. Plot of chemical data from the intrusives around Valis on a) Rb/Nb versus Y/Nb (Eby, 1992) and b) Ga/Al *10000 versus Nb diagrams (Whalen et al, 1987). The data are plotted in the A type granite field.

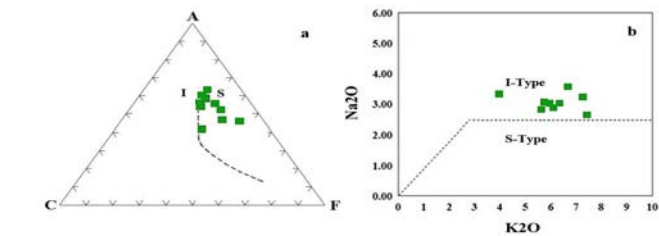


Figure 4. Plot of chemical data from the intrusives around Valis on a) ACF (Chappell and White, 1992) and, b) Na2O versus K2O diagrams (Chappell and White, 1974). The data from the study area are consistent with both I and S granites.

Plotting the data on the granitoid tectonomagmatic discrimination diagrams (figure 8) shows that they usually fall within the WPG fields.

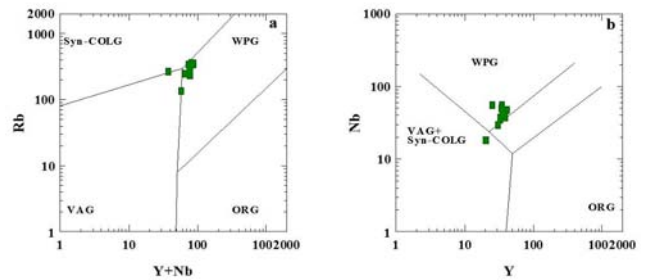


Figure 8. Plot of chemical data from the study area's intrusives on a) Rb-(Y+Yb) and b) Nb-Y diagrams (Pearce et al, 1984). These data usually plot in the WPG field.

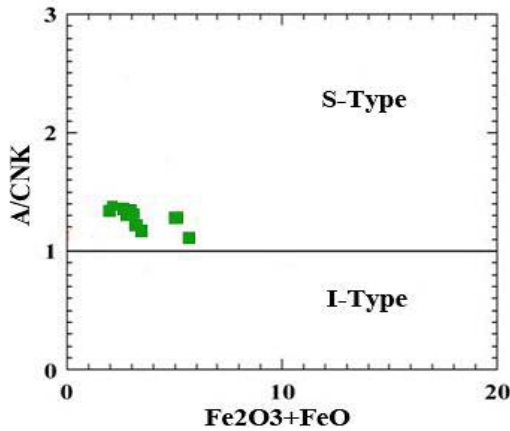


Figure 5. The chemical data from the intrusives around Valis plot in the S field on the ACNK-Fe2O3+FeO diagram (Pearce et al, 1984).

Using Geochemical Features to Study the Mineralization Potential of the Intrusives around Valis

Determining the mineralization potential of felsic intrusive bodies is important because every specific type of granite is usually accompanied with a specific type of ore deposit. For example, paligenetic granites have mineralization potential for Cu, Au, Nb and minor amounts of Sn and W (Beus, 1968). High amounts of Li, Rb compared to K (lower K:Rb ratio) and Sr compared to Rb (high Rb:Sr ratio) are geochemical characteristics of magmatic production that can be used to study the separation of volatile substances and magmatic rare metals from magma, increasing the mineralization potential (Beus, 1968).

Special indicator minerals can indicate the economic concentrations of some metallic rare elements; for example, the existence of tourmaline and topaz in granitoid bodies can imply tin mineralization as cassiterite. In addition, pink, robellite type tourmalines are abundant in lithium bearing pegmatites (Rozendaal et al, 1995); therefore, the economic value and mineralization type of the pegmatites can be partially recognized according to the color of the existing tourmalines (Beus, 1968). Aplite can be seen in some granite bodies in the study area, especially in marginal zones or in the veins that form across the bodies. These aplites have tourmalines that are black in hand specimen. On the other hand, there is no sign of topaz; therefore, the mineralization of tin is unlikely.

Tungsten has different distributions in barren and fertile intrusives. In a few samples from barren igneous bodies, the W content is higher than 5 ppm, and no sample is observed with W content higher than 10 ppm. However, at least 10% of the samples from fertile bodies contain more than 10 ppm of tungsten (Jonasson and Boyle 1972). The intrusive bodies, which have been affected by post magmatic hydrothermal processes (Jonasson and

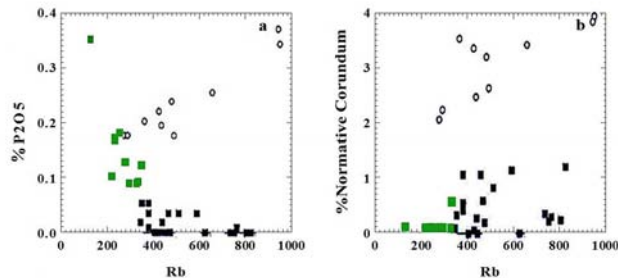


Figure 6) Plot of chemical data from the intrusives around Valis on a) normative corundum versus Rb and b) P2O5 versus Rb diagrams for I (solid squares) and S type (hollow circles) granites related to the Lachlan Fold Belt in Australia (Pearce et al, 1984). The data from the study area are consistent with both I and S granites.

Boyle, 1972). The amount of this element in the study area's intrusives ranges from 1.4 to 5.9; therefore, they are barren in terms of W.

The degree and type of differentiation and oxidation state of the magmas that formed granites are important to determine the potential and type of associated mineralization (Blevin, 2003). The K/Rb ratio is used to determine the transition state of granite melts; if the ratio is under 100, the granite is highly evolved (Rossi et al, 2011) (figure 9). This observation occurs because Rb tends to be differentiated in the melt during the segregation stage of aqueous liquid phases from the remaining silicate melts (Clarke, 1992). This ratio ranges from 142.8 to 271.4 in the study area's intrusives. The average value of K/Rb in the intrusives around Valis (table 3) is higher than all the values in table 4; according to this table, the greater the mineralization in the granitoid bodies the lower the ratio is, as Rb tends to remain in the melts and be differentiated among the silicate melts and aqueous liquids. Therefore, these granitoids are not strongly differentiated; in other words, the granite melts that created the intrusives in the study area are insufficiently evolved (table 4). Thus, the aforementioned bodies have not undergone sufficient post magmatic activity to cause mineralization. The value of K/Rb in the study area's intrusives is similar to the average for granitoids unrelated to Li, Be, Sn, W and Ta ore deposits, so the intrusives are classified as barren granites (table 4). The evolved nature of the granites is also recognizable using the Sr-Rb-Ba triangular diagram by El Bouseily & El Sokhary (1975) (figure 10). Most samples plot in the normal granite field, which shows that the intrusives in the study area are not completely evolved.

The ratio of compatible to incompatible elements (such as Sr/Rb) is also a useful tool to recognize the differentiation type of granite magmas (Blevin 2003, Ishihara and Tani 2004, Blevin and Chapell, 1992) (figure 11); in particular, the granite magmas in the study area have been slightly differentiated. Bea et al (2006) suggested another index to recognize the evolution of magmas; if $Zr/Hf < 20$, strong magmatic hydrothermal alteration has occurred, while if $Zr/Hf > 20$, magmatic hydrothermal alteration has not occurred. The Zr/Hf ratio in the study area's intrusives is between 33.8 and 44.4; therefore, magmatic hydrothermal alteration has not occurred.

The Sm/Eu and Rb/Ba ratios and amounts of Rb, Ba and Sr in the intrusives around Valis are higher than those of the S type granite source rocks of porphyry tin deposits around the world (Rongfupei and Dawei Hog, 1995; Lehmann et al, 1989) (table 5). Diagrams using the aforementioned parameters can show the fertility of the granitoids with respect to Sn (Karimpour, 1999); accordingly, the intrusives in the study area lack tin mineralization (figure 12a and b).

To discriminate granitoids and recognize their economic potential for tin, molybdenum or porphyry copper, the Rb/Sr and Ce/Yb ratios and color index (obtained from $[Cl=(SiO_2+K_2O+Na_2O)/(MgO+CaO+FeO)]$) can be used (Karimpour et al, 1983) (figure 13a and b). Tin, high grade and low-grade molybdenum and porphyry copper deposits have been completely discriminated in these diagrams. The chemical data imply that the intrusives in the study area are barren in Sn and Mo but somewhat fertile in Cu (especially sample B7).

The geochemical behaviors of the copper and zinc in magnetic crystallization products are different. Unlike copper, which is found in the chalcopyrite phase, zinc replaces iron in iron and magnesium silicates. In intermediate rocks (with 52 to 60 wt% silica), the amount of zinc is fixed at approximately 85 ppm. In rocks with over 60% silica, the zinc amount decreases linearly with increasing SiO₂. In rhyolite with 75% SiO₂, the amount reaches 35 ppm (Wolf, 1975). Wolf believed that practically all rocks with total iron higher than 10% can be used in regional explorations of zinc. Considering prior research and using the SiO₂ versus Fe and Zn diagrams by Wolf (1975), we recognize the barren nature of the study area's intrusive bodies with respect to zinc (Figure 14).

Table 3. Average of the rare and major elements in the intrusives around Valis.

Element	K (%)	Rb (ppm)	Sr (ppm)	Ba (ppm)	Zr (ppm)	Hf (ppm)	Eu (ppm)	K/Rb	Ba/Rb	Rb/Sr	Zr/Hf
Average	4.9	259	269	517.75	369	10.82	0.89	189.43	1.99	0.962	34.1

Table 4. K/Rb ratios of barren and fertile granites (Beus, 1968) compared to those in the intrusives around Valis.

Type of Granitoid	K/Rb
Average of the granitoids	170
Average of the granitoids unrelated to Li, Be, Sn, W and Ta deposits.	170
Average of the granitoids related to Li, Be, Sn, W and Ta deposits.	130
Average of the biotite granites related to Li, Be, Cs and Ta pegmatitic deposits.	160
Average of the biotite granites related to Ta pegmatitic and apogranitic deposits.	126
Average of the granitoids in the study area.	189/43

Table 5. Amount and ratios of some rare elements in S type granites around the world that contain tin compared to the intrusives in the study area (Not Analyzed = NA).

Mine's Name	Sr _(ppm)	Ba _(ppm)	Rb _(ppm)	Sm/Eu	Rb/Ba
China, Yanbei granites	23-18	65-35	1100-800	25	25-16
South of China, Yanyan granites	NA	NA	NA	18	NA
Southeast of China, Gianlishan granites	35	35	4300-3600	65-20	21
Southeast of China, Yoaganixian granites	NA	NA	NA	75	NA
Southeast of China, Xihuashan granites	NA	NA	NA	45	NA
Australia, Blue Tier batholith	31-9	35	543-1500	35-20	15
Australia, Emuford Herberton region	19-5	35-5	700-500	120-40	100-20
Brazil (northeast), Maderia granites	20	32	5100-670	95-15	115-33
Southwest of Japan, Sanyo	20	25	350	70-50	17
Thailand, Thai-Barmese granites	9-1	85-38	2570-1100	NA	55-30
South of Thailand, Phuket Island, Kato body	44-9	85-20	1390-680	NA	75-30
The intrusives around Valis	492-199	1293-236	347-131	10.78-4.12	1.4-0.2

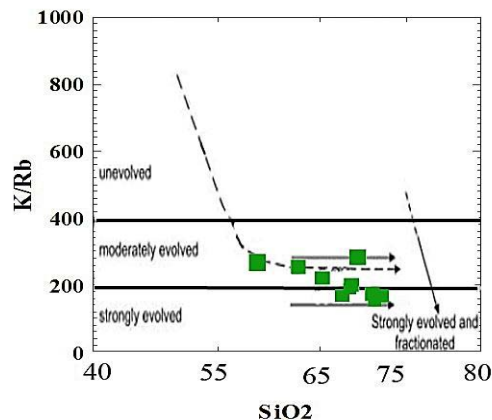


Figure 9. Plot of K/Rb versus SiO₂ (Blevin, 2003). The study area's intrusives are semi-evolved.

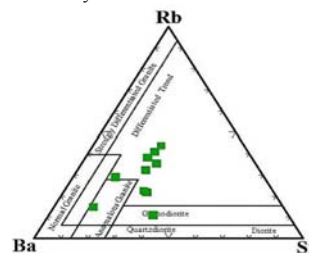


Figure 10. Plot of the study area's samples on Sr, Rb and Ba triangular diagram (El Bouseily and El Sokhary, 1975).

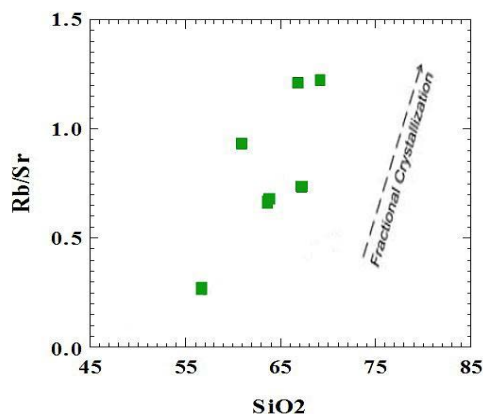


Figure 11. Diagram of Rb/Sr versus SiO₂ (Blevin, 2003) and a plot of the study area's samples.

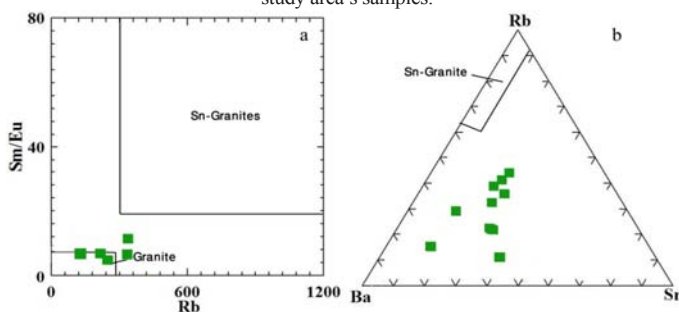


Figure 12. Plot of the study area's intrusives on a) Sm/Eu versus Rb and b) Rb-Ba-Sr diagrams, which discriminate tin-bearing granites from barren ones (Karimpour et al., 1983).

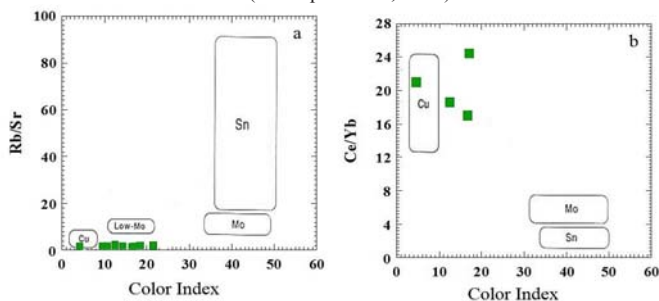


Figure 13. The discrimination source rock diagrams of Cu, Sn and Mo porphyry deposits using a color index and ratios of a) Rb/Sr and b) Ce/Yb (Karimpour, 1999), and a plot of the study area's samples.

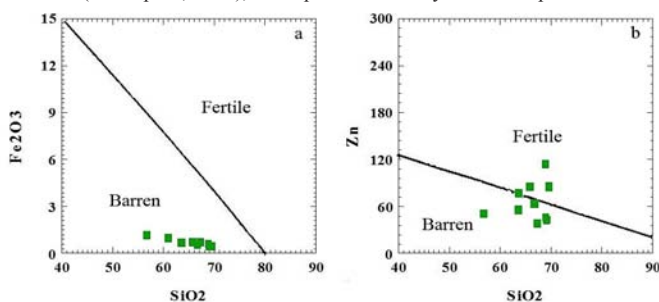


Figure 14. The relationship between changes in a) Fe and b) Zn versus SiO₂ in barren and fertile granites (Wolf, 1975), and a plot of the data related to the study area.

Results

Based on the information obtained from field studies and the petrography and analysis results of the intrusives around Valis, the following results are determined:

1 - These intrusives have granite, syenite and monzonite petrographic compositions (granitoid) and are mostly metaluminous.

2 - Contradictory features in the intrusives (such as the behavior of P, Rb, Ga/Al, Y/Nb, K/Na, and FeO/Fe₂O₃, the Rb/Nb ratios, the A/CNK molar ratios and the A/CNK-Fe₂O₃+FeO and ACF diagrams), some of which are consistent with the I nature and others with the S and A natures, show that the rocks are classified as hybrid granitoids.

3 - In terms of the tectonomagmatic setting, the rocks are classified as WPG granitoids.

4 - Based on the K/Rb ratio, these granitoids are not strongly differentiated and have not undergone post magmatic activity, which would lead to mineralization. The amount of K/Rb in the study area's intrusives is similar to the average of granitoids unrelated to Li, Be, Sn, W and Ta deposits, classifying the intrusives as barren granites.

6 - The Sm/Eu and Rb/Ba ratios and the behavior of Rb, Ba and Sr in the intrusives around Valis are completely different compared to the S type granite source rocks of porphyry tin deposits around the world and are barren in terms of tin.

7 - The chemical data (Rb/Sr, Ce/Yb ratios and color index) imply that the intrusives in the study area are barren in terms of Sn and Mo but are somewhat fertile in Cu.

8 - The changes in Zn and Fe versus SiO₂ show the barren nature of these intrusives.

References

- Alavi, M. (1996) Tectonostratigraphy synthesis and structural style of the Alborz Mountain system in northern Iran. *Geodynamics Journal*, 21, 1–33.
- Bea, F., Montero, P. and Ortega, M. (2006) A LA-ICP-MS evaluation of Zr reservoirs in common crustal rocks: implications for Zr and Hf geochemistry, and zircon forming processes. *The Canadian Mineralogist*, 44, 693–714.
- Beus, A. A. (1968) *Geochemical criteria in theoretical principles of exploration for mineral deposits*, Moscow, PP. 127-145.
- Blevin, P. (2003) *Metallogeny of granitic rocks*, The Ishihara Symposium, *Granites and Associated Metallogeneses*, 14, 5–8.
- Blevin, P. L. and Chappell, B. W., (1992) The role of magma sources, oxidation states and fractionation in determining the granite metallogeny of eastern Australia. *Transaction of the Royal Society of Edinburgh: Earth Sciences*, 83, 305–316.
- Chappell, B. W. and White, A. J. R., (1974) Two contrasting granite types. *Pacific Geology*, 9: 173-174.
- Chappell B. W., White A. G. R. (1992) I and S type granites in the Lachlan fold belt, *Transactions of the Royal Society of Edinburgh Sciences*, 83, 1-26.
- Clarke, D. B. (1992) *Granitoid Rocks*: Chapman and Hall, pp. 238.
- Cox K. G., Bell J.D., Pankhurst R.J. (1979) *The interpretation of igneous rocks*, Allen and Unwin, London, 405 p.
- Davis, R. G., Jones, C. R., Hamzepour B. and Clark, G. C. (1972) *The Geology of the Musuleh sheet (Northwest Iran)*: Geol. Survey of Iran, Report No. 24, 110 pp.
- Eby, G. N., (1992) Chemical subdivision of the A-type granitoids, petrogenetic and tectonic implications, *Geology* 20, 641-644.
- El Bouseily, A. M. and El Sokkary, A. A. (1975) The relation between Rb, Ba and Sr in granitic rocks, *Chemical Geology*, 16, 207–219.
- Haj Ailou, B. (2000) *Metallogeny of tertiary in western Alborz-Azerbaijan (Miyaneh-Siyahroud) with specific view on Hashtjin area*, PhD thesis, Shahid Beheshti University.
- Ghorbani, M. (2013) *The economic Geology of Iran Mineral Deposits and Natural Resources*, Springer, 569 pp.

- Irvine, T. N., Baragar, W. R. A. (1971) A guide to the chemical classification of the common volcanic rocks, *Can. J. Earth Sc.*, 523-548.
- Ishihara, S. and Tani, K. (2004) Magma mingling/mixing v. magmatic fractionation: Genesis of the Shirakawa Mo-mineralized granitoids, Central Japan, *Resource Geology*, 54, 373–382.
- Jonasson, I. R. and Boyle R. W. (1972) Geochemistry of mercury and origins of natural contamination of the environment, *Can. Inst. Min. Metall. Bull.*, 65 (717): 32-39.
- Karimpour, M.H. (1999) Application of Sm/Eu, Rb/Sr, Ce/Yb and F-Rb ratios to discriminate between tin mineralized and non-mineralized S-type granite, *Journal of earth sciences*, Iran.
- Karimpour, M.H, and Bowes, W.W. (1983) Application of trace elements and isotopes for discriminating between porphyry molybdenum, copper, and tin systems and the implications for predicting the grade: *Global Tectonics and Metallogeny*, V. 2, No. 1, 2, pp. 29-36.
- Lehmann B. and Mahawat C. (1989) Metallogeny of tin in Central Thailand: A genetic Concept, *Geology*, P.D., and Piccoli, P.M, 1989, Tectonic discrimination of granitoids: *Geol. Soc. of Am. Bull.*, V. 101, p. 635-6430.
- Maniar, P. D. and Piccoli P. M. (1989) Tectonic discrimination of granitoids, *Geological society of America Bulletin*, 101: 635-643.
- Moayyed, M., 2001, Petrologic study of Tertiary volcano-plutonic belt in western Alborz, Azerbaijan, Ph.D. Thesis, Shahid Beheshti University
- Pearce, J.A., Harris, N.B.W., Tindle, A.G., (1984) Trace element discrimination diagrams for the tectonic interpretation of granitic rocks, *J. Petrol.*, 25, 956-983.
- Peyrovan, H., (1992) Petrographic, petrologic and geochemical studies of intrusive rocks north of Abhar and the association of plutonism in the area with mineralization, MSc thesis, Tarbiyat Moalem University.
- Rongfu Pei and Dawei Hog (1995) the granites of south China and their metallogeny: *Episodes: Vol. 1&2*, pp. 77-82.
- Rossi, J. N., Toselli, A. J., Basei, M. A., Sial, A. N. and Baez, M. (2011) Geochemical indicators of metalliferous fertility in the Carboniferous San Blas pluton, Sierra de Velasco, Argentina, in: Sial, A. N., Bettencourt, J. S., De Campos, C.P. & Ferreira, V. P. (eds) *Granite-Related Ore Deposits*, Geological Society, London, Special Publications, 350, 175–186.
- Rozendaal, A., and Bruwer, L. (1995) Tourmaline nodules: mineralization in the Cape Granite Suite, South Africa. *Journal of African Earth Sciences*, 21, 141–155.
- Torkamani, E., (1997) Petrologic study of intrusive rocks north of Abhar-Khoramdarreh. MSc thesis, Shahid Beheshti University
- Whalen, J. D., Currie, K. L., and Chappell, E. W. (1987) A-type granites: geochemical characteristics, discrimination and petrogenesis, *cont. Min. Pet.*, 95, 407-419.
- Wolf, M. B., (1975) Estimation of parameters affecting rapid fluid transfers in the whole body, isotopic infusions, *Ann. Biomed Eng.*, 3: 209-224.